THE CHARACTERIZATION OF NICKEL-DOPED TIO_2-BASED DYE SENSITIZED SOLAR CELLS USING NATURAL DYES EXTRACTED FROM *PERSEA AMERICANA L*, *MURRAYA KOENIGII*, *CITRUS SINESIS L* AND *TALIUM FRUTICOSUM* LEAVES

SANDRA ONYEKA MALUMI[*,1], ARTHUR EKPEKPO[2], OBED OYIBO[3], PRECIOUS OKEOGHENE ANTHONY[4]

[1,3,4] Department of Physics, Delta State University of Science and Technology, Ozoro.
[2]Department of Physics, Delta State University, Abraka.

*Corresponding author: sandraom@dsust.edu.ng +2347068155441

ABSTRACT

This study concentrates on the third generation photovoltaic cell, which is the conventional dye-sensitized solar cell. This type of solar cell is generally made up from various components such as photo anode support, photo sensitizer (dye), electrolyte and counter electrode. In this research, Nickel was used to doped TiO_2 with Avocado leaf (*Persea Americana L*), Currry leaf (*Murraya koenigii*), Orange leaf (*Citrus sinesis L*) and Ceylon spinach (*Talium fruticosum*) for DSSCs fabrication. The sensitized TiO_2/silver with dye recorded an efficiency of 0.47%, 0.47%, 0.05%, and 0.04% for Avocado leaf (*Persea Americana L*), Curry leaf (*Murraya koenigii*), Orange leaf (*Citrus sinesis L*) and Ceylon spinach leaves (*Talium fruticosum*) respectively. *The optical energy bandgap was observed to be 2.32 eV for* TiO_2 *and 3.50 eV, 3.51 eV, 3.51 eV, and 3.52 eV*. The structure of the cells is polycrystalline, with several noticeable peaks at 24.891°, 27.509°, 30.375° ,32.915°, 27.509°, 35.296°, 38.814°, 43.152°, 47.579°, 53.231° and 59.130° for TiO_2 and 21.689°, 26.363°, 28.162°, 30.464°, 30.083°, 33.083°, 35.780°, 40.612°, 45.207°, 49.387° and 54.466° for $TiO_2/Ni_{0.1}$/avocado leaf, $TiO_2/Ni_{0.1}$/curry leaf and $TiO_2/Ni_{0.1}$/orange leaf corresponding to (101), (004), (200), (105), (211), (204), (116), (220), (215) and (303) planes, respectively. The structure of cells is polycrystalline and exhibit the highest peak (200) at 30.375, (211) at 33.083, (200) at 28.162 and (105) at 30.622 for the bare TiO_2 and$TiO_2/Ni_{0.1}$/avocado leaf, $TiO_2/Ni_{0.1}$/curry leaf and $TiO_2/Ni_{0.1}$/orange leaf, respectively.

Keyword: Photovoltaic, Dope, Photo sensitizer, Band gap energy.

Introduction

Finding new energy sources with the least amount of toxicity has been one of the biggest challenges of the past ten years (Hosseinnezhad *et al*., 2013). The sun is Earth's most abundant source of renewable and clean energy (Etula, 2012). According to the pioneering work by Gratzel (O'Regal and Gratzel, 1991) there have been proposals for devices that use dye-sensitized solar cells (DSSCs) to convert the energy from the sun into electrical energy. Compared to silicon based solar cells, DSSC photovoltaic technology is less expensive and more environmentally friendly (Mahmood *et al*., 2015). Natural dye-sensitized solar cells, or NDSSCs for short, are becoming more and more popular because of their low manufacturing costs and environmentally benign characteristics (Hug et al., 2014). Extensive research has been done for the enhancement of the photo conversion efficiency (Malumi *et al*., 2023). Ruthenium dyes, free metal organic dyes, and natural dyes are examples of photosensitizers, which are essential components of DSSCs that have a significant effect on efficiency (Berginc *et al.*, 2008).

With current technology, DSSC can convert photons from sunlight with an efficiency of 13% to electrical energy (Mattew, 2014). In order to create more stable and effective cells, a great deal of work has gone into optimizing the many DSSC components (Malumi *et al*. 2023). A redox couple electrolyte system, usually an iodide or triiodide complex, is positioned between two glass plates together with a photo-anode and a counter electrode to form the DSSC as it is shown in Figure 1. The oxidized dye is replenished by the electrolyte's redox couple. The photo-anode is composed of a monocrystalline semiconductor (titanium dioxide, TiO_2) doped with nickel (II) chloride ($NiCl_2$) that acts as a framework for the dye sensitizer and a glass plate coated with a thin layer of transparent conductive oxide (fluorine doped tin-oxide, FTO). In order to catalyze the redox reaction with electrolyte, the counter electrode is also composed of a glass slide covered in FTO and typically coated with a small layer of carbon. Recent research has focused a great deal of effort on doping elements into DSSC photoanodes. More dye molecules can be adsorbed in the working electrode as a result of the greater surface area brought about by increased roughness and pores following doping, which enhances performance and raises the conversion efficiency of TiO_2 electrode-based DSSC (Arunachalam *et al*., 2016).

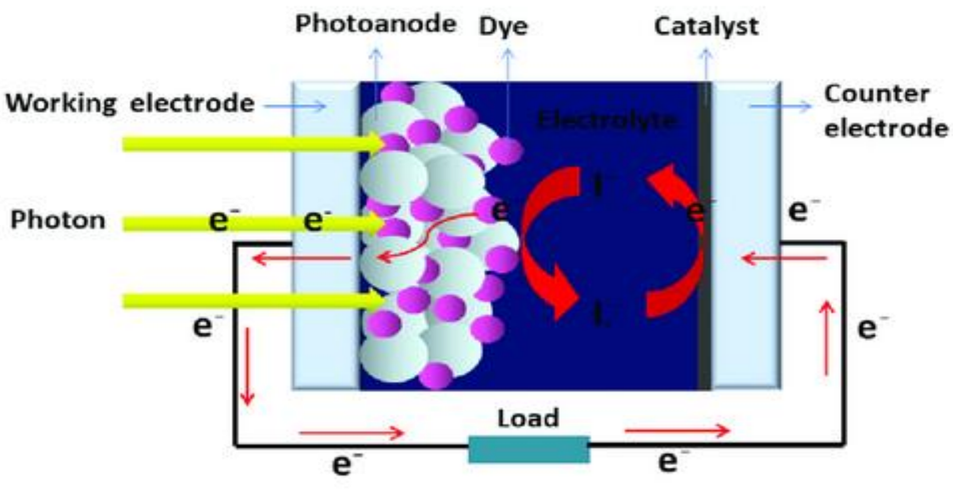

Figure 1: Basic structure of a Dye-Sensitized Solar Cell (DSSC) (Nurmaeimah *et al.*, 2018)

The majority of fruits, flowers, and leaves naturally display a variety of colors and contain several pigments that can be readily extracted and used in DSSCs (Calogero and Marco, 2018). Most green plants possess a great deal of chlorophyll in their leaves, and numerous studies have examined at using this pigment as a natural dye (Gratzel, 2003; Tennakone *et al.*, 1996; Zhang *et al.*, 2008). In this research, chlorophyll extracts of Avocado leaf (*Persea Americana L*), Curry leaf (*Murraya koenigii*), Orange leaf (*Citrus sinesis L*) and Ceylon spinach (*Talium fruticosum*) were the natural dyes used as dye-sensitizers for the fabrication of DSSCs.

*Persea Americana L (*Avocado) leaves are small to medium in size and oblong to eplliptic In shape, averaging 4-10 cm wide and 10-30 cm in length. The surface on the top of the leaf is dark green and leathery, while the bottom of the leaf is matte and light green to brown. In Nigeria, it is locally known as Ewé pia in Yoruba language, Akwukwo Ube oyibo in Igbo, Ganyen piya in Hausa and uberoyibo in Urhobo Language. Originally from Asia, Murraya koenigii is a tropical to sub-tropical tree of the Rutaceae family. It can also be found in Nigeria. Curry leaves are small in size and long, slender, oval in shape narrowing to a point, averaging to 2-4cm in length and 1-2cm in width. Curry leaf is a delicious, aromatic shrub which is widely used as spice, condiments and also used to treat various diseases (Maheswari *et al*., 2018). It commonly called ufuo-yibo (Urhobo), nchanwu (Igbo), efirin oso (Yoruba) and marugbo sanyan (Hausa). Orange trees have rounded crowns, branched growth, and alternately oriented oval or elliptical leaves on their branches. It belongs to the family of Rutaceae. Orange leaf is light green in color with a texture that stays the same throughout the entire length. It is locally called Oroma in Igbo, Utien in Urhobo language (Dickson *et al*., 2012). *Talinum triangulare* (Ceylon Spinach) is a green vegetable that can be eaten that is part of the family *Portulaceae.* Water leaf plant grows erect, reaching a height of 30 to 100cm. it bears small, pink flowers and broad, fleshy leaves (Bioltif and Edward, 2020). It is commonly known as Gure in Yoruba, Mgbolodi in Igbo and Alenyruwa in Hausa.

Experimental Details

Extraction of Dyes from plant leaves

Fresh leaves of Avocado leaf (*Persea Americana L*), Curry leaf (*Murraya koenigii*), Orange leaf (*Citrus sinesis L*) and Ceylon spinach (*Talium fruticosum*) was harvested, selected at random from the local Agricultural farms within Delta, Nigeria. The leaves were rinsed thoroughly with purified water and air dried until they became invariant in weight for two weeks at a room temperature range of 24 ^{o}C – 32 ^{o}C. The leaves were ground using an electric blender to form a powder of which 50 g of each ground leaf was measures using a weighing scale and put in a 500 ml beaker. They were soaked with 100 ml of methanol and stirred on a magnetic stirrer for 3hours, then covered with an aluminum foil sheet and set aside for 24 hours. The dyes from the leaves are then extracted into a beaker by the help of filter paper. The filtered samples are poured into storage containers and kept out of reach of the sun rays. This is to prevent degradation of the dyes (Senthil *et al*., 2014).

Preparation of substrate (FTO glass)

In order to eliminate any dust or contamination that might have remained on the substrate after manufacture, the FTO glass was cleaned prior to cell fabrication by submerging it in an ultrasonic bath for roughly 30 minutes in each of the acetone and distilled water solutions. To help remove the acetone that was initially put on the substrate and the components that the acetone did not clear, another 20 minutes of ultrasonic bathing are conducted using methanol. In order to prepare the substrate for deposition, it was finally heated to 50°C using a hot air oven.

Preparation of the photoanode Deposition on FTO glass

The TiO_2 thin film electrode (photoanode) was made by the Doctor Blade technique. The word "Doctor Blade" describes a method of smoothing films that applies or removes liquid substance from another surface using any type of blade steel, rubber, plastic, or another (Kontos *et al.* 2008, Tian *et al*. 2010). The TiO_2 paste was prepared by the addition of 5 ml of methanol to 3 g of TiO_2 powder drop wise in a mortar while grinding and stirring with a pestle to separate aggregated particles of TiO_2 mechanically. During the process of the cell fabrication 0.1 mol nickel (II) chloride ($NiCl_2$) were used to dope the TiO_2, the nickel (II) chloride ($NiCl_2$) were dissolved with 2 ml of methanol before adding to the TiO_2 paste.

A transparent fluorine-doped tin oxide (FTO) conducting glass with average dimension 2.25 cm by 2.35 cm was used as substrate for the deposition of TiO_2/ nickel (II) chloride ($NiCl_2$) paste. An ohmmeter was used to check for the conductive side on the glass. Two transparent FTO conducting glasses were used during the deposition. While one is the depositing surface, the other is used as a guide to ensure uniformity. Paper tape was applied on the conductive side to mask 0.15 cm – 0.2 cm at the three edges of the depositing glass surface and the opposite sides of the guiding slide. A glass rod is used to ensure that there is no opening into the masked edges. After evenly distributing drops of the TiO_2 colloidal solution onto the substrate, the material was smeared with a glass stirring rod. The grown films were annealed at 250°C for 30 minutes using a thermostatic blast resettable oven with a temperature range of 50°C to 1000°C. After which it was kept to cool and ready for sensitization.

Dye loading

During sensitization process, nickel (II) chloride ($NiCl_2$) coated glass films were separately immersed for about 24 hours in the various dye extracts. The stained TiO_2/ nickel (II) chloride ($NiCl_2$) film is removed using a thong and the sample is placed on a rack with the stained surface facing up.

Preparation of counter electrode

The counter electrode was made from another conductive glass. An ohmmeter was used to check for the conductive side on the glass. A pencil made of carbon is used to coat the conductive side of the glass substrate. No masking or tape was required for this electrode, and thus the whole surface was coated to increase its surface area. The Potassium Iodide-Iodine electrolyte solution from Institute of Chemical Education (ICE) was used as redox electrolyte.

Assembly of DSSC and electrical output measurement

Each dye stained nickel (II) chloride ($NiCl_2$) electrode was placed on a laboratory table such that the film side faced up, and the counter electrode was placed on top so that the conductive side of the counter electrode made direct contact with the TiO_2/ nickel (II) chloride ($NiCl_2$) film. The two opposing glass slides were offset such that the entire TiO_2/ nickel (II) chloride ($NiCl_2$) was covered by the counter electrode, and the 0.2 cm strip of glass not coated by TiO_2/silver nickel (II) chloride ($NiCl_2$) was exposed. Two crocodile clips were used to hold the slides together at the other edges. Potassium Iodide-Iodine (KI/Iodine) electrolyte solution was injected through the edges of the slides. The completed solar cell was taken for measurements so as to determine the current-voltage characteristics.

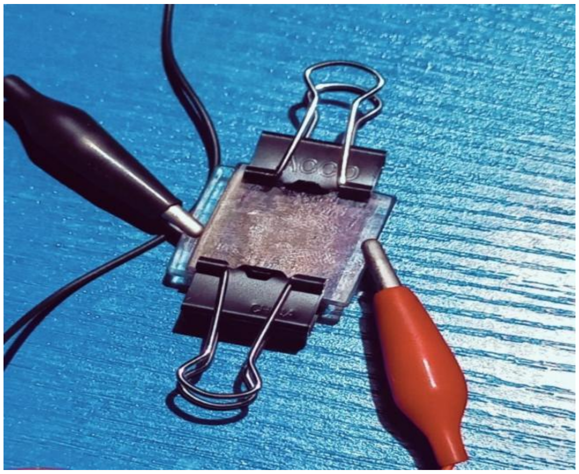

Figure 2: Showing the fabricated solar cell undergoing electrical testing

Film Characterization

Optical Characterization of films

The film were characterized for their optical properties using UV-VIS-NIR (UV-1800 series) Schimadzu spectrophotometer in the wavelength range of 200 – 1100 nm. This was done to check for the absorbance, reflectance, transmittance, refractive index, co-efficient of absorption, optical thickness, energy band gap, optical conductivity of the natural dyes used in the sensitization of the substrate. This can also be done by substituting either the absorbance reflectance or transmittance values into the various equations (1-9) listed below;

$$A + T + R = 1 \quad (1)$$

Where A is the absorbance, R is the reflectance and T is the transmittance, given by

The transmittance (T) is related to absorption (A) by the expression (Filip *et al.*, 2012):

Absorption, $A = 2 - Log(\%T)$ (2)

Where %T is the percentage of light transmitted

Transmittance, $T = 10^{A}$ (3)

Reflectance, $R = 1 - (A + T)$ (4)

The refractive index (n) = $\frac{1}{Ts} + \sqrt{\frac{1}{Ts^{-1}}}$ (5)

Where Ts is the percentage transmittance.

$$\text{Optical thickness (t)} = \frac{ln\left(\frac{1-R^2}{T}\right)}{\alpha} \tag{6}$$

Where R is the reflectance, T is the transmittance and α is the absorption coefficient

Experimentally, absorption coefficient (α) can be calculated from the simple relation (Al-ofin *et al.*, 2012):

$$Absorption\ coefficient, \alpha = \frac{1}{\mathrm{d}} \ \mathrm{In}\left(\frac{1}{\mathrm{T}}\right) \tag{7}$$

Where t is the thickness of the thin film, T and R are the transmittance and reflectance respectively.

The band gap energy (E_g) of the transparent films is determined by using the equation (Yousaf and Abass, 2013):

$$\alpha hv = A(hv - E_g)^2 \tag{8}$$

A is a constant that depends on the properties of the material, α is the absorption coefficient, hυ is the photon energy and n is a constant, equal to ½ for a direct band gap semiconductor. The energy band gap of the materials will be obtained by extrapolating the linear part of the curve $(ahv)^2 = 0$ in a graph of $(ahv)^2$ against hv.

$$\text{Optical conductivity}, (\sigma) = \frac{\propto nc}{4\pi} \tag{9}$$

Where α is the absorption coefficient, n is the refractive index, c is the speed of light.

Morphological Characterization of DSSC

The surface morphological characteristics and elemental analysis of the TiO_2 photoanode were investigated using a Scanning Electron Microscopy (SEM) and Energy dispersive X-ray spectroscopy (EDS), respectively.

Structural Characterization of DSSC

The structural characterization of the dyes were obtained to study the crystal structure and element spacing of the dyes used in the sensitization of the cells by the use of a X-ray diffraction (XRD) (Cu-$K_{\alpha 1}$ radiation source, λ = 1.5406Ǎ). The data generated was used to calculate several structural factors, including crystallite size, dislocation density, d- spacing, and lattice parameters a and c. The crystallite size of the thin films was calculated by XRD patterns using Debye Scherrer's formula in equation (10) (Maurya *et al.*, 2018).

$$D = \frac{K\lambda}{\beta cos\theta} \quad (10)$$

Where D is the crystallite size, k is a constant given as 0.94, λ is the X-ray wavelength used, β is the full width half maximum (FWHM) of the XRD peak appearing at the diffraction angle θ. is the angle of diffraction.

The dislocation density δ which gives more information on the number of defects in the films was determined by eqn. (11) (Dixit *et al.*, 2019).

$$\delta = \frac{1}{D^2} \quad (11)$$

The lattice parameter (a and c) of the films were calculated using equation (12) and (13) respectively (Bindu and Thomas, 2014).

$$a = \frac{\lambda}{\sqrt{3}\sin\theta} \quad (12)$$

$$c = \frac{\lambda}{\sin\theta} \quad (13)$$

The inter-planar spacing was calculated using the relation (Hossain *et al.*, 2018),

$$d_{hkl} = \frac{n\lambda}{2\sin\theta} \quad (14)$$

Where n is the order of diffraction which is usually 1, λ is the X-ray wavelength and θ is the Bragg diffraction angle at peak position in degrees.

Electrical characterization of sensitized film

The electrical properties of the fabricated DSSC was evaluated by the use of a solar simulator and digital source meter readings which gives the open-circuit voltage (V_{oc}), short-circuit current (I_{sc}). The current and voltage characterization of the DSSC will be studied and from the I-V characteristics, the fill factor (FF) and the photo conversion efficiency (PCE) were obtained.

I. **Open-circuit voltage (V_{oc}):**
The open-circuit voltage (V_{oc}) voltage is the measured cell voltage when there is no current flow within the cell. It is the highest voltage a solar cell can produce when there is no resistance between the working and counter electrodes. This represents the difference between the redox potential of the electrolyte and the Fermi level of the semiconducting oxide.

II. **Short-circuit current (I_{sc})**

The short circuit current is the output current of the cell when the voltage difference between the electrode is zero. In other words, it is the current obtained from the cell when the load resistance is zero. Usually, it is presented in terms of the short circuit density (I_{sc}), which is the ratio between the measured short-circuit current.

III. **Fill factor (FF)**

This represents the relationship between the maximum power output (Pm) and the sum of the open-circuit photovoltaic (Voc) and short-circuit photocurrent (Isc). The fill factor ff can then take values between 0 and 1. This represents the extent of the electrical and electrochemical losses occurring during the operation of the DSSCs.

Hence,

$$FF = \frac{Pm}{(\text{Isc x Voc})} = \frac{I_m \times V_m}{(I_{sc} \times V_{oc})} \quad (15)$$

Where I_{sc} and V_{oc} is the photocurrent and photovoltage to the maximal power point (Pm) respectively.

IV. Photo- conversion efficiency (PCE)

The photo-conversion efficiency (Ƞ) measures the efficiency of the conversion of incident light into electrical energy (Bera *et al.*, 2021).

$$\eta = \frac{Isc \text{ x Voc x FF}}{pin} \times \frac{100}{1} \quad (16)$$

Where Isc, Voc, FF and Pin are the short circuit current density, the open –circuit voltage, the fill factor and the incident light power intensity respectively.

Result and discussion

Optical absorption analysis was performed with a UV-VIS-NIR (UV-1800 series) Schimadzu spectrophotometer. The optical diagrams above shows the absorbance, transmittance, reflectance and energy band gap for plant dyes used as sensitizers. These natural extracts absorbed in the visible region of light spectrum and fulfilled the criterion for the use of photosensitizer in the dye-sensitized solar cell. Figure 3 shows the absorbance spectra of TiO_2 and $TiO_2/Ni_{0.1}$/dyes extracted from the leaves of avocado, curry, orange and Ceylon spinach. The decrease in absorbance is associated with an increase in wavelength. The dye-sensitized material exhibits an absorption broad band of 630-700 nm in the visible light region indicating the absorption of red light from the photons. More noticeable peak of absorption was observed at 680 nm, 680 nm, 660 nm and 650 nm for all four dye extract, with dye extract of Avocado leaves having most noticeable peak. Since all the dyes used in this research are chlorophyll-based, the absorption spectra appear to be similar. The spectra exhibited by all the dyes were found to be similar with the data reported for chlorophyll-based photosensitizer and is the reason for the efficient harvesting of photons in natural DSSC (Syafinar *et al.*, 2015; Mattew, 2016). Plant parts containing chlorophyll have been widely investigated for use as photosensitizers in the fabrication of natural DSSC (Kabir *et al*., 2019; Sullano and Sia, 2018; Arof and Ping, 2017). In addition to their high absorption coefficient in the visible region of the electromagnetic spectrum, the presence of CHO anchoring groups on chlorophyll enable their adsorption unto the surface of the TiO_2. Matthew in 2016 noted that chlorophylls absorb light energy strongly in the red region of the absorbance spectrum, while reflecting green. The presence of nickel as a dopant led to a drop in enhancement of the absorbance characteristic compared to the absorbance peak noticed when silver nitrate ($AgNO_3$) was used to doped cells (Malumi *et al.*, 2023). The peaks in the avocado and curry leaf dye display suggest that they are suitable for further dye studies. Fabricated cells are the optimum solution for solar and other light-emitting applications.

The transmittance spectra of TiO_2 and $TiO_2/Ni_{0.1}$/dyes are illustrated in Figure 4. This shows that an increase in wavelength result to an increasing transmittance. The dye-sensitized material displays a surge ranging from 635 to 710 nm in the visible light region, which is evidence of the cell's acceptance of both the nickel and dye. The surge which is clearly visible, suggests that the cell has transmitted all light wavelength ranging from 300-1100 nm, exempting red light which shows the least transmittance with range 640 -700 nm. The dye-sensitized material peaked at different wavelengths, i.e., 665 nm, 670 nm, 670 nm, and 670 nm for Avocado, curry, orange and Ceylon spinach leaves, respectively. Avocado and curry leaf dye peaks show potential for further dye studies.

Figure 5 shows the reflectance analysis of TiO_2 and $TiO_2/Ni_{0.1}$/dyes. Reflectance increases alongside wavelength. The presence of nickel and dye in the cell of the dye-sensitized material can be observed as a minor peak in the visible light range. When exposed to light, nickel and dye increase the energy storage capacity of the material, enabling the cell to absorb more energy. The highlighted peak indicates nickel and dye. The cells' reflectance characteristic was enhanced by nickel as a dopant. The potential for future dye studies is indicated by the peaks in avocado and curry leaf dye. The most effective solution for solar and other light-emitting applications are fabricated cells.

Figure 6 shows how to estimate the energy bandgap of dye-sensitized material and TiO_2 and $TiO_2/Ni_{0.1}$/dyes *by extending the straight part of the Tauc plots. Since the absorption coefficient (α) can be stated, this can be accomplished as*

$$\alpha h v = \left(hv - E_g\right)^{1/2} \qquad (17)$$

Where Eg, hv, *α and A are the energy bandgap, photon energy, absorption coefficient and constant respectively and the intercept on the horizontal axes gives a good estimation to the optical energy bandgap. From the result, the optical energy bandgap was observed to be 2.23 eV for* TiO_2 *and 3.50 eV, 3.51 eV, 3.51 eV, 3.52 eV for* avocado leaf, curry leaf, orange leaf, and Ceylon spinach dye respectively.

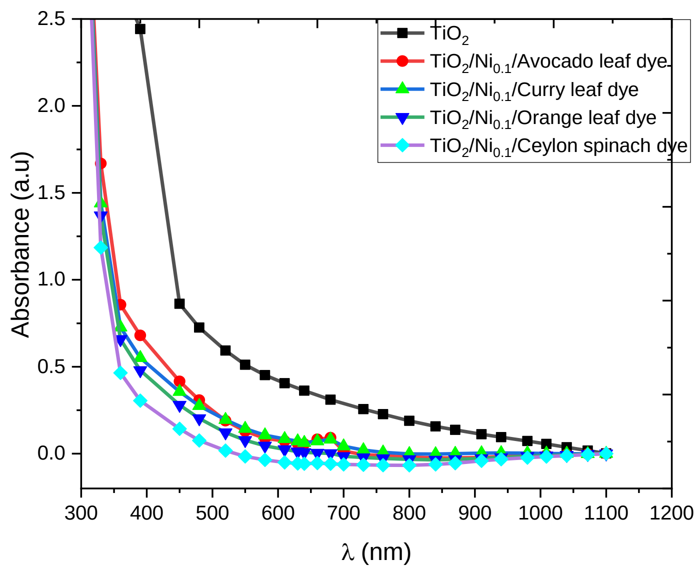

Figure 3: Absorbance spectra of dyes extracted from Avocado leaf (*Persea Americana L*), Curry leaf (*Murraya koenigii*), Orange leaf (*Citrus sinesis L*) and Ceylon spinach (*Talium fruticosum*) as sensitizers. The absorbance of TiO_2 films is also shown for comparison.

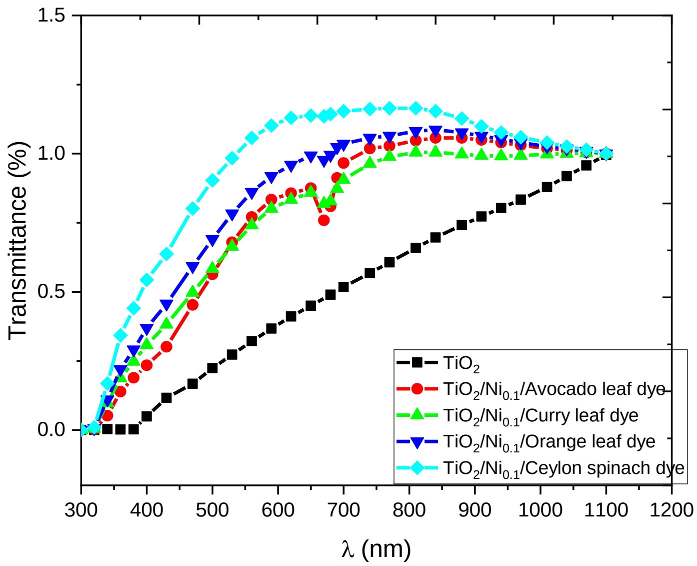

Figure 4: Transmittance spectra of dyes extracted from Avocado leaf (*Persea Americana L*), Curry leaf (*Murraya koenigii*), Orange leaf (*Citrus sinesis L*) and Ceylon spinach (*Talium fruticosum*) as sensitizers. The transmittance spectrum for TiO_2 films is also shown for comparison.

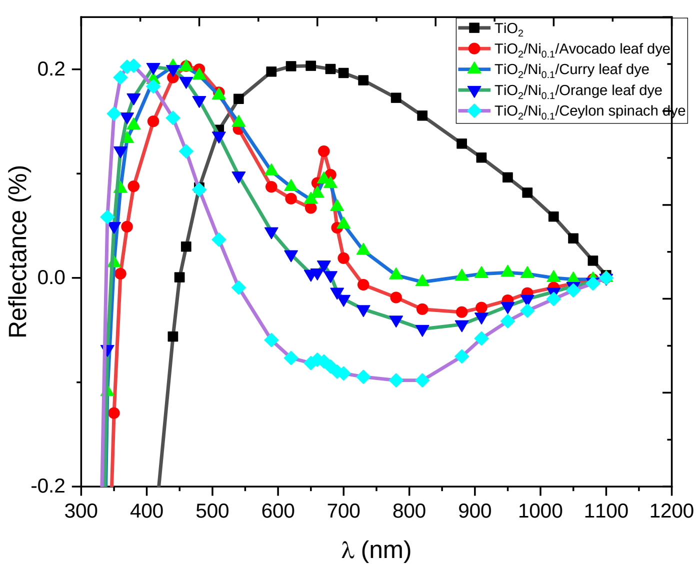

Figure 5: Reflectance spectra of dyes extracted from Avocado leaf (*Persea Americana L*), Curry leaf (*Murraya koenigii*), Orange leaf (*Citrus sinesis L*) and Ceylon spinach (*Talium fruticosum*) as sensitizers. The reflectance spectrum for TiO_2 films is also shown for comparison.

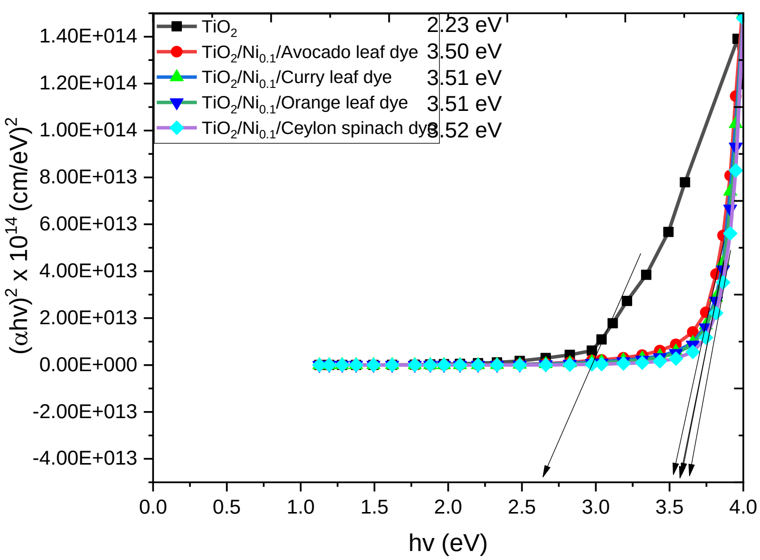

Figure 6: The determination of energy band gap of dyes extracted from Avocado leaf (*Persea Americana L*), Curry leaf (*Murraya koenigii*), Orange leaf (*Citrus sinesis L*) and Ceylon spinach (*Talium fruticosum*) as sensitizers. The energy level for TiO_2 films is also shown for comparison.

5. Scanning Electron Microscopy (SEM) Results of the TiO_2 mesoporous layers

The surface morphological characteristics and elemental analysis of the TiO_2 photoanode were investigated using a Field-Emission Scanning Electron Microscopy (SEM) (JSM 7100F, JEOL.COM) at a magnification of 20.0 kx and view field of 10.4 µm and Energy dispersive X-ray spectroscopy (EDS), respectively. Figure 7 displays the surface morphology of synthesized TiO_2 and $TiO_2/Ni_{0.1}$/dyes. The surface of TiO_2 exhibits a few clouded nanoparticles showing a nano growth in the micrograph. The FTO substrate has a good deposition of TiO_2 synthesis on its surface. The surface energy of TiO_2 experienced a complete change following the deposition of dye and nickel (Ni).The micrograph of avocado leaf dye in the film showed a shift in the surface of the synthesized material from clouded nanoparticles to nano pebble. The surface micrograph of curry leaf dye shows that the nano cluster sticks to the surface of the substrate. In the micrograph, the substrate is covered with nanoparticles and nanoflakes of orange leaf dye that are tightly adhering. TiO_2, silver, and dye enhance the surface energy of the synthesized material for solar and photovoltaic uses. The thickness of TiO_2 on the FTO glass was found to be about 102 nm and $TiO_2/Ni_{0.1}$/dyes film was found to be approximately 109.35 nm, 109.00 nm, 108.23 nm and 110.64 nm respectively.

The EDX spectrum of the synthesized TiO_2 and $TiO_2/Ag_{0.1}$/dyes is shown in Figure 8 was carried out to determine the elements present in the material. The synthesized FTO showed distinguished peaks of titanium, oxygen, silicon and calcium in the bare TiO_2 and $TiO_2/Ag_{0.1}$/dyes mesoporous film. Titanium (Ti) having the greatest peak followed by oxygen (O), corresponding to the major elements present in the bare TiO_2. The peaks shown in the figure represents the level of concentration of the various elements present. The presence potassium, calcium, carbon, Aluminum, sodium and silver content, at lower concentration in the $TiO_2/Ag_{0.1}$/dyes shows the thorough absorption of the dye and dopant. It is evident from the spectrum that all the elements composing TiO_2 mesoporous film are present.

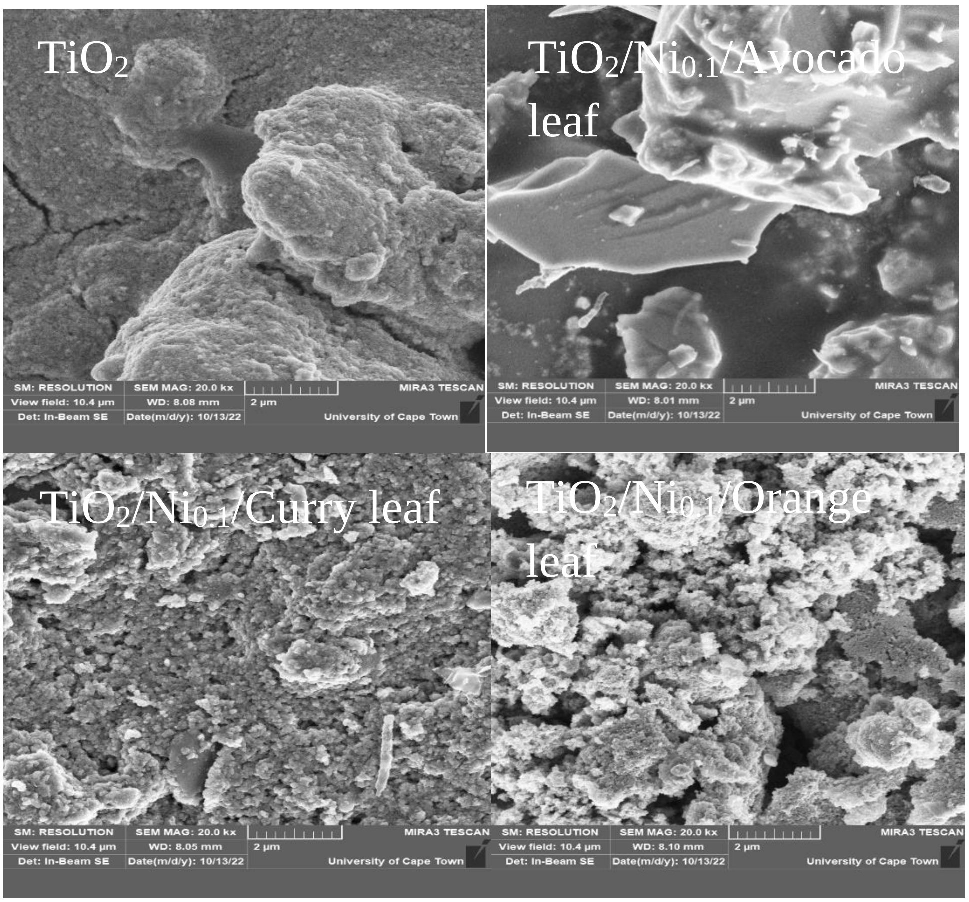

Figure 7: SEM micrograph of TiO_2 and $TiO_2/Ni_{0.1}$/dyes

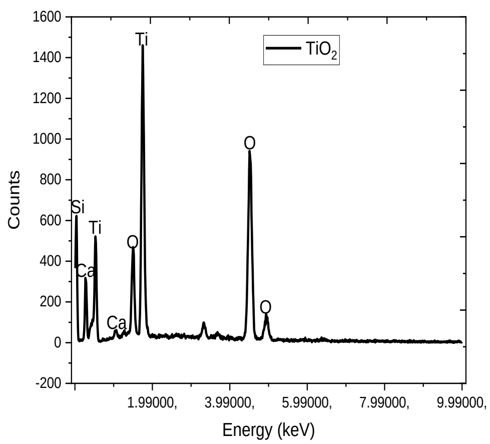

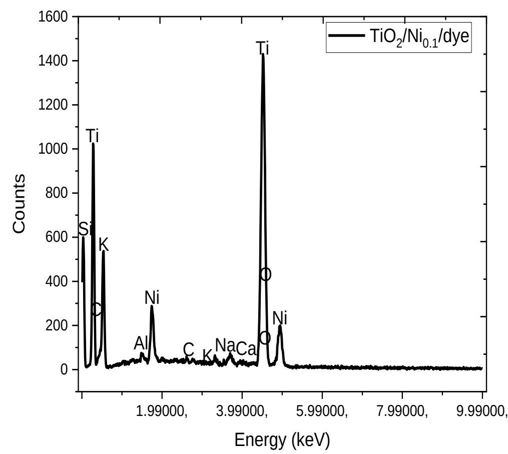

Figure 8: EDX spectrum of TiO_2 and TiO_2 /$Ni_{0.1}$/dyes

X-Ray Diffraction Structural Results of the TiO_2 mesoporous layers

Figure 9 displays the XRD analysis results for the synthesized TiO_2 and TiO_2/$Ni_{0.1}$/dye. Ten peaks at 24.891°, 27.509°, 30.375° ,32.915°, 27.509°, 35.296°, 38.814°, 43.152°, 47.579°, 53.231° and 59.130° for TiO_2 and 21.689°, 26.363°, 28.162°, 30.464°, 30.083°, 33.083°, 35.780°, 40.612°, 45.207°, 49.387° and 54.466° for TiO_2/$Ni_{0.1}$/avocado leaf, TiO_2/$Ni_{0.1}$/curry leaf and TiO_2/$Ni_{0.1}$/orange leaf corresponding to (101), (004), (200), (105), (211), (204), (116), (220), (215) and (303) planes, respectively. The structure of cells is polycrystalline and exhibit the highest peak (200) at 30.375, (211) at 33.083, (200) at 28.162 and (105) at 30.622 for the bare TiO_2 andTiO_2/$Ni_{0.1}$/avocado leaf, TiO_2/$Ni_{0.1}$/curry leaf and TiO_2/$Ni_{0.1}$/orange leaf, respectively. Improved crystal structure and energy absorption on TiO_2's lattice parameters led to higher peak intensity. The crystals' energy absorption didn't affect the peak locations. Due to the dye, there is a distortion in the lattice structure and individual cells, which causes shifts in crystal orientation. The crystallinity of the films is enhanced by increased grain size for TiO_2,TiO_2/$Ni_{0.1}$/avocado leaf, TiO_2/$Ni_{0.1}$/curry leaf and TiO_2/$Ni_{0.1}$/orange leaf. The grain size was calculated using the Debye-Scherrer equation (Maurya *et al.*, 2018);

$$D = \frac{0.94\lambda}{\beta\cos\theta} \tag{1}$$

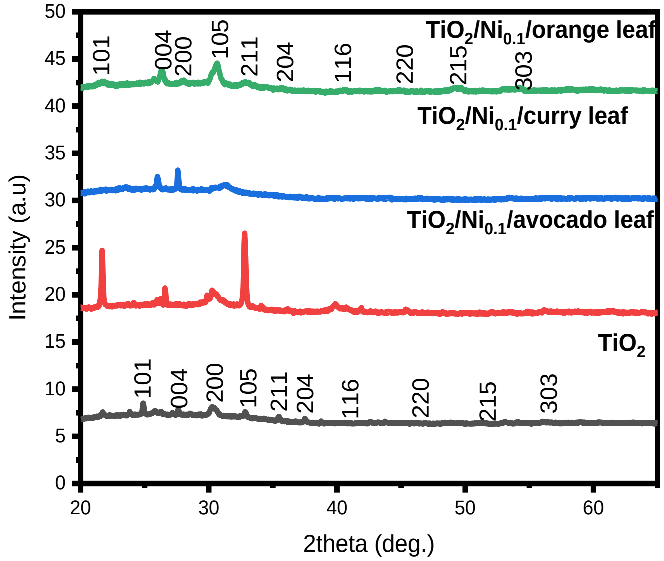

Figure 9: XRD pattern of TiO_2 and$TiO_2/Ni_{0.1}$/dye

Table 1: Structural variables for the synthesized films

Films	2θ (°)	d-spacing (Å)	FWHM	(hkl)	Lattice constant a (A)	Dislocation density (δ)	Grain Size (D) nm
TiO_2	24.891	3.573	0.109	101	6.190	1.795	1.302
	27.509	3.239	0.112	004	6.478	1.875	1.274
	30.375	2.939	0.113	200	5.879	1.884	1.271
	32.915	2.718	0.114	105	6.079	1.893	1.268
	35.296	2.540	0.117	211	6.222	1.969	1.243
	38.814	2.317	0.119	204	6.556	1.996	1.235
	43.152	2.094	0.120	116	5.924	1.973	1.242
	47.579	1.909	0.123	220	6.332	2.007	1.231
	53.231	1.719	0.127	215	5.955	2.042	1.221
	59.130	1.560	0.129	303	5.840	1.994	1.235
$TiO_2/Ni_{0.1}$/avocado L.	21.689	4.093	0.010	101	7.090	1.528	1.411
	26.363	3.377	0.011	004	6.755	1.817	1.294
	28.162	3.165	0.012	200	6.331	2.146	1.191
	30.622	2.916	0.013	105	6.522	2.491	1.105
	33.083	2.705	0.014	211	6.626	2.853	1.033
	35.780	2.507	0.016	204	7.091	3.673	9.106
	40.612	2.219	0.021	116	6.277	6.146	7.040

	45.207	2.003	0.022	220	6.646	6.536	6.826
	49.387	1.843	0.023	215	6.386	6.919	6.635
	54.466	1.683	0.023	303	6.297	6.626	6.780
TiO_2/ $Ni_{0.1}$/curry L.	21.689	4.093	0.015	101	7.090	3.438	9.411
	26.363	3.377	0.023	004	6.755	7.946	6.191
	28.162	3.165	0.024	200	6.331	8.586	5.956
	30.622	2.916	0.025	105	6.522	9.212	5.750
	33.083	2.705	0.026	211	6.626	9.842	5.563
	35.780	2.507	0.027	204	7.091	1.046	5.396
	40.612	2.219	0.021	116	6.277	6.146	7.040
	45.207	2.003	0.022	220	6.646	6.536	6.826
	49.387	1.843	0.023	215	6.386	6.919	6.635
	54.466	1.683	0.025	303	6.297	7.829	6.237
TiO_2/ $Ni_{0.1}$/orange L.	21.689	4.093	0.017	101	7.090	4.417	8.304
	26.363	3.377	0.021	004	6.755	6.624	6.781
	28.162	3.165	0.022	200	6.331	7.215	6.497
	30.622	2.916	0.023	105	6.522	7.797	6.250
	33.083	2.705	0.024	211	6.626	8.386	6.026
	35.780	2.507	0.025	204	7.091	8.968	5.828
	40.612	2.219	0.022	116	6.277	6.745	6.720
	45.207	2.003	0.023	220	6.646	7.143	6.530
	49.387	1.843	0.024	215	6.386	7.533	6.358
	54.466	1.683	0.025	303	6.297	7.829	6.237

Photovoltaic Results of the fabricated DSSC's

The natural dye extracted from the plant dyes (as sensitizer) was performed by measuring the I-V (the current voltage) curve under light. The test was performed with the use of equipment called Solar Simulator connected to the source. The interpretation was done quantitatively by a computer with lab trace software. The performance of the natural dye is evaluated by I_{sc} (short circuit current),V_{oc}(open circuit voltage), Fill Factor (FF) as well as the conversion efficiency (η).

The photovoltaic performance of DSSCs fabricated using Avocado, curry, orange leaves and Ceylon spinach dyes as a potent sensitizer for $TiO_2/Ni_{0.1}$ was assessed. The result obtained via the current, voltage, fill factor and conversion efficiency measurement is displayed in Table 2. The result revealed that the curry and avocado leaf dye sensitizer efficiency is greater than that of the orange leaves and Ceylon spinach dyes. After optimization of the photoanode and counter electrode, a photoelectric conversion efficiency (η) of 0.47 %, 0.47 %, 0.05 %, 0.04 %; an open-circuit voltage (Voc) of 0.0.510 V, 0.500 V, 0.376 V, 0.365 V, and a short-circuit current density (Isc) of 1.427 mA/cm^2, 0.407 mA/cm^{2,} 0.239 mA/cm^2, 0.245 mA/cm^2. The cell with highest efficiency among this group of DSSC is the cell sensitized with curry with PCE of 0.47% in comparison with the result recorded by Rosana *et al.* in 2019, having an efficiency of 0.27 %. The reason for such low efficiency recorded in orange leaves and Ceylon spinach dye was due to the fact that the presence of the $NiCl_2$ tends to reduce the absorbance of energy from the sun by the dye.

Table 2: The Photovoltaic performance of the TiO_2 mesoporous film sensitized by natural dye.

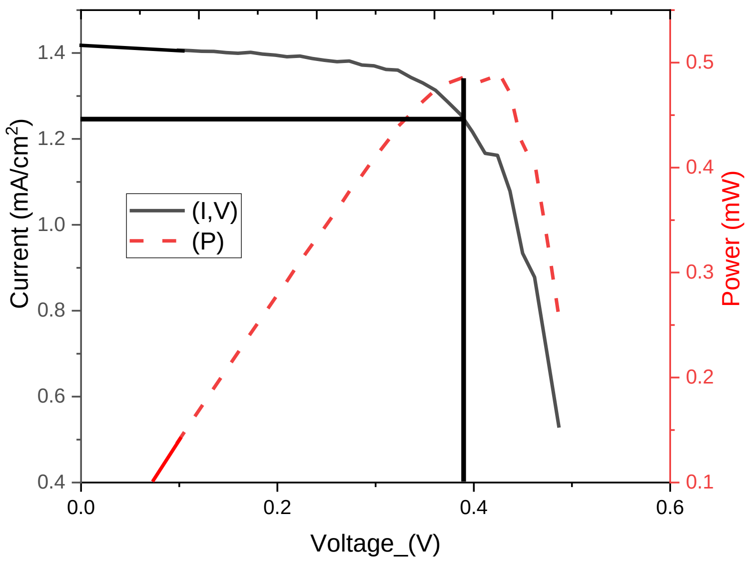

Figure 10: I-V curve of DSSC sensitized with the dye extract from *Persea Americana L (Avocado leaf)*

Sensitized TiO_2 mesoporous films	**V_{oc} (V)**	**I_{sc} (mA/cm^2)**	**V_{max} (V)**	**I_{max} (mA/cm^2)**	**P_{max} (mWcm^{-2})**	**Fill Factor, FF**	**Efficiency, η (%)**
$TiO_2/Ni_{0.1}$/Avocado leaf dye	0.510	1.427	0.380	1.242	0.471	0.65	0.47
$TiO_2/Ni_{0.1}$/Curry leaf dye	0.500	0.407	0.384	1.225	0.480	2.31	0.47
$TiO_2/Ni_{0.1}$/Orange leaf dye	0.376	0.239	0.211	0.243	0.051	0.57	0.05
$TiO_2/Ni_{0.1}$/Ceylon spinach dye	0.365	0.245	0.244	0.182	0.044	0.49	0.04

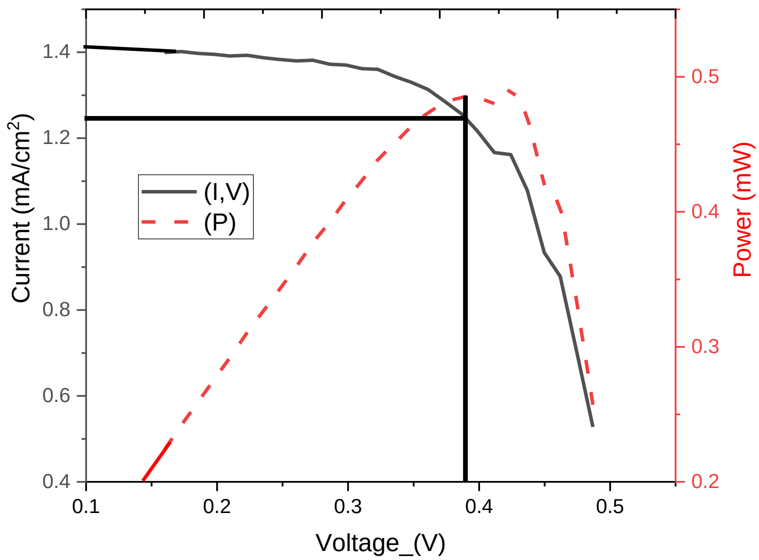

Figure 11: I-V curve of DSSC sensitized with the dye extract from *Murraya koenigii* (curry leaf)

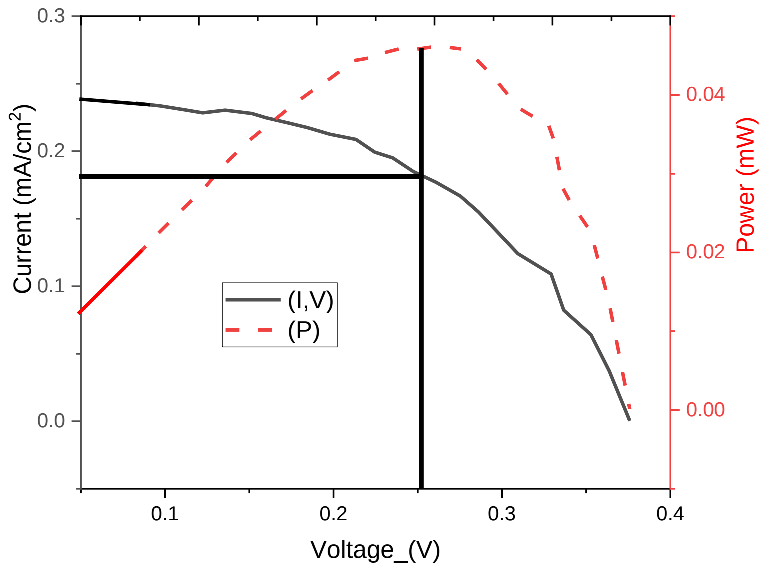

Figure 12: I-V curve of DSSC sensitized with the dye extract from *Citrus sinesis L* (orange leaf)

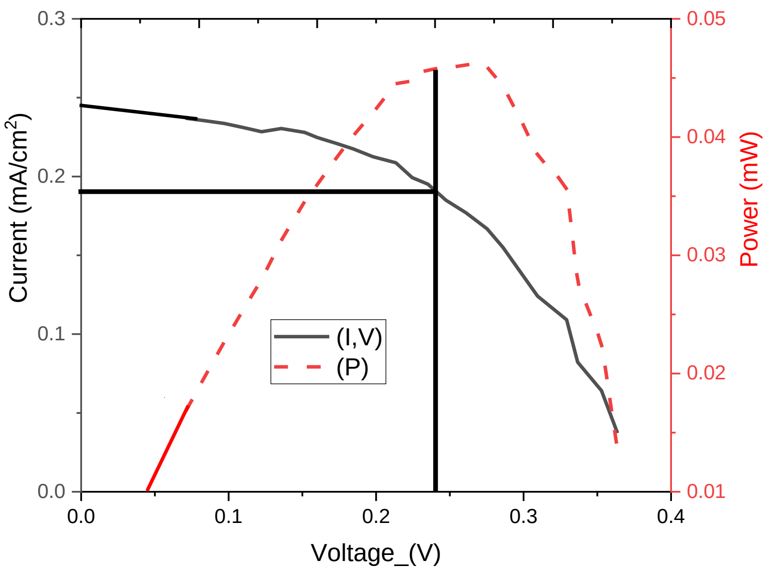

Figure 13: I-V curve of DSSC sensitized with the dye extract from *Talium fruticosum* (Ceylon spinach)

Conclusion

The sensitization of an affordable, sustainable dye solar cell using extract of Avocado leaf (*Persea Americana L*), Curry leaf (*Murraya koenigii*), Orange leaf (*Citrus sinesis L*) and Ceylon spinach (*Talium fruticosum*) leaves has successfully been fabricated. The optical, morphology, structural and electrical properties of the Nickel doped dyes/TiO_2 coated FTO glass was investigated via UV-VIS spectroscopy, scanning electron microscopy and energy-dispersive x-ray spectroscopy. The plant leaf dyes absorbs visible light in the range of 630-700 nm, thereby allowing red visible light to pass through in significant amount. Other visible transmit through the dye except for the green light which is been reflected back as shown in the reflectance spectra with a prominent peak of 670 nm. The photovoltaic energy conversion efficiency fabricated DSSCs are 0.47 %, 0.47 %, 0.05 % and 0.04 % respectively. The cell with the highest efficiency is the cell sensitized with the dye extract of Avocado leaf and curry leaf extract with V_{oc} of 0.510 V , 0.500 V and I_{sc} of 0.427 mA / cm^2 and 0.407 mA / cm^2 having the lowest energy band gap value of 3.50 eV and 3.51 eV which shows the highest peak of absorption.

References

Al-ofin, H.H., Abdel-Raheem, M. M. & Ateyyah, M.A. (2012). Structural and optical properties of fluorine-doped of Al2ZnO4 thin films deposited by D.C. sputtering technique. *Journal of non-oxie glasses, 3*(3), 39-54.

Arunachalam, A., Dhanapandian, S. & Manoharan, C. (2016). Effect of Sn doping on the structural, optical and electrical properties of TiO_2 films prepared by spray pyrolysis. *Physical Electronics, 76*, 35–46.

Bera, S., Sengupta, D., Roy, S. & Mukherjee, K., (2021). Research int dye sensitized solar cells: a review highlighting progress in India. *Journal of Physics: Energy, 3*(03), 521-560. https://doi.org/10.1088/2515-7655/abff6c

Bioltif, Y.E & Edward, N.B. (2020). Review on the Medicinal Potentials of Waterleaf (Talinum triangulare). *Mediterranean Journal of Basic and Applied Sciences (MJBAS), 4*(2), 01-07.

Calogero, G. & Marco, G.D. (2008). Red Sicilian Orange and Purple Eggplant Fruits as Natural Sensitizers for DyeSensitized Solar Cells. *Solar Energy Material Solar Cell, 92*(11), 1341-1346. doi:10.1016/j.solmat.2008.05.007

Etula, J. (2012). Comparison of three Finnish berries as sensitizers in a dye−sensitized solar cell. *Eur. J. Young Sci. Eng. 1*, 77–84.

Gratzel, M. (2003). Dye-Sensitized Solar Cell. *Journal of Photochemistry & Photobiology C: Photochemistry Reviews, 4*(2), 145-153. doi:10.1016/S1389-5567(03)00026-1

Hossein, B. M. (2010). Performance of nano structured dye-sensitized solar cell-utilizing natural sensitizer operated with platinum and carbon coated counter electrode. *International Journal of Chemistry Tech Research, 1*(2), 615-619.

Hosseinnezhad, M., Moradian, S. & Gharanjig, K. (2013). Synthesis and application of two organic dyes for dyesensitized solar cells. *Prog. Colour Colorants Coat. 6*, 109–117.

Hug, H., Bader, M., Mair, P. & Glatzel, T. (2014). Biophotovoltaics: Natural pigments in dye-sensitized solar cells Appl. Energy 115, 216–225.

Kabir, F., Bhuiyan,M.M.H., Manir, M.S., Rahaman, M.S., Khan, M.A. & Ikegami, T. (2019). Development of dye sensitized solar cell based on combination of natural dyes extracted from Mabalar spinach and red spinach. ELSEVIER: Physics 14. https://doi.org/10.1016/j.rinp.2019.102474

Kontos, A. I., Kontos, A.G., Tsoukleries, D.S., Bernard, M.C., Spyrellies, N. & Falaras, P., (2008). Sensitizers performance of dye sensitized solar cell. *Journal of materials processing technology, 196*(4), 243-248.

M. Berginc, U. Opara−Krasorec, & M. Hocevar, "Perfor− mance of dye−sensitized solar cells based on Ionic liquids: Effect of temperature and iodine concentration", Thin Solid Film. 516, 7155–7159 (2008).

Maheswari, B., Dhanpal, C. & Lakshmi, B. (2018). A review on curry leaves (Murraya koenigii): versatile multi-potential medicinal plant. *International Journal of Advances in Pharmacy Medicine and Bioallied Sciences*, *6*(1), 31-41.

Mahmood, A., Hussain Tahir, M., Irfan, A. Al-Sehemi, A.G. & Al−Assiri, M.S. (2015). Heterocyclic azo dyes for dye sensitized solar cells: A quantum chemical study. *Comput. Theory. Chem. 1066*, 94–99.

Malumi, S.O., Malumi, T., Osiele, M.O., Ekpekpo, A. & Ikhioya, I.L (2023). Enhance And Performance Evolution Of Silver-Doped Titanium Dioxide Dye Sensitized Solar Cells Using Different Dyes. *Journal of Engineering in Industrial Research*, *4*(4), 189-200.

Mary Rosana, N. T., Joshua, A. D & Vincent, J. K. L. (2014). Natural green pigment to transform sunlight into electricity.*Journal of Chemical and Pharmaceutical Research*, 7, 1517.

Mathew, S. (2014). Dye-sensitized solar cells with 13% efficiency achieved through the molecular engineering of porphyrin sensitizers. *Nat. Chem. 6(1)*, 242–247.

Mathew, S., Yella, A., Gao, P., Humphry-Baker, R., Curchod, B., Ahari-Astani, N., Tavernelli, I., Rothlisberger, U., Nazeeruddin, M.K. & Gratzel, M. (2014). Dye-sensitized solar cells with 13% efficiency achieved through the molecular engineering of porphyrin sensitizers. *Nature Chem* ***6***, 242–247. https://doi.org/10.1038/nchem.1861

Matthew, P.J. (2016). Photosynthesis. *Essays in Biochemistry*, *60*,255–273 DOI: 10.1042 /EBC 20160016

Maurya, I.C., Singh, S., Neetu, Gupta, A.K., Srivastava, P. & Bahadur, L. (2018). Dye-sensitized solar cells employing extracts from four Cassia flowers as natural sensitizers: studies on dye ingredient effect on photovoltaic performance. *Journal of Electronic Material Science*, *1*(47), 225–232. https://doi.org/10.1007/s11664-017-5759-3.

Maurya, I.C., Singh, S., Neetu, Gupta, A.K., Srivastava, P. & Bahadur, L. (2018). Dye-sensitized solar cells employing extracts from four Cassia flowers as natural sensitizers: studies on dye ingredient effect on photovoltaic performance. *Journal of Electronic Material Science*, *1*(47), 225–232. https://doi.org/10.1007/s11664-017-5759-3.

Nurnaeimah, J., Mohamad, I.S., Norizan, M.N. & Mahmed, N. (2018). Enhancement of Energy Conversion Efficiency for Dye Sensitized Solar Cell using Zinc Oxide Photoanode. *IOP Conference Series: Materials Science and Engineering*, *374* 012048.

O'Regan, B. & Gratzel, M. (1991). A low cost, high efficiency so− lar cell based on dye−sensitized colloidal TiO2 films. *Nature, 353*, 737–740.

Rosana, N.T., Amarnath, J., Kumar, P.S. & Vincent, J. (2019). Potential of plant-based photosensitizers in dye-sensitized solar cell applications. *Journal of Environmental Progress and Sustainable Energy*, *39*(3).

Senthil, T., Muthukumarasamy, N. & Kang, M. (2014). ZnONanorods Based Dye Sensitized Solar Cells Sensitized using Natural Dyes Extracted from Beetroot, Rose and Strawberry. *Bulletin of the Korean Chemical Society*. *35*(4), 1050-1056.

Sullano, M.T. & Sia, R.C. (2018). Dye sensitized solar cell with nut grass (Cyperus rotundus) leaves, Malabar spinach (Basella alba) buds and Mayana (plectranthus scutellarioides) leaves extracts as photosensitizers. Journal *of Scientific International (Lahore), 30*(2), 239-242.

Syafinar, R., Gomesh, N., Irwanto, M., Fareq, M. & Irwan, Y. (2015). Chlorophyll pigments as nature based dye for dye-sensitized solar cell (DSSC). *Energy Procedia*, *79*(6),896-902.

Tennakone, K., Kumara, G., Kumarasinghe, V.P., Sirimanne, M. & Wijayantha, K. G. U. (1996). Efficient Photosensitization of Nanocrystalline TiO_2 Films by Tannins and Related Phenolic Substances. *Journal of Photochemistry & Photobiology A: Chemistry, 94*(2), 217-220. doi:10.1016/1010-6030(95)04222-9

Tian, H., Hu, L., Liu, W., Huang, Y., Guo, L., Mo, L., Sheng, J., & Dai, S., (2010). Retarded charge recombination in dye sensitized nitrogen doped TiO_2solar cells. *Journal of Physical chemistry*, 114(627).

Yousaf, S.A. & Abass, J.M. (2013). Structural, Morphological, and optical characterization of SnO2: F thin films prepared by chemical spray pyrolysis. *International Letters Chemistry Physics and Astronomy*, *13*(2), 90-102.

Zhang, D., Lanier, S. M., Downing, J. A., Avent, J.L., Lumc, J. & McHale, J.L. (2008). “Betalain Pigments for DyeSensitized Solar Cells,” *Journal of Photochemistry Photobiology A: Chemistry*, 195(1), 72-80. doi:10.1016/j.jphotochem.2007.07.038